JOURNAL OF MATERIALS SCIENCE 18 (1983) 785–792

Strength and fatigue of multicomponent optical glass fibres

P. W. FRANCE, W. J. DUNCAN, D. J. SMITH, K. J. BEALES
British Telecom Research Laboratories, Martlesham Heath, Ipswich, Suffolk, UK

Strength and fatigue of multicomponent glass fibres have been measured as a function of environment and glass composition. Strength and dynamic fatigue were measured using a two-point bending technique from − 196 to 100° C and also in vacuo down to 10^{-5} torr. Zero stress ageing and static fatigue have been measured in ambient air and water at 20° C for different glass compositions. The addition of zinc, magnesium and aluminium oxides to sodium borosilicate glasses were shown to give significant improvements to the corrosion behaviour and a glass has been developed which could survive in water for longer than 7×10^3 h at strains greater than 1%. Finally a modified theory of static fatigue has been outlined in order to explain the departure from conventional stress corrosion theory that was evident in some glass compositions.

1. Introduction

There has been a considerable amount of research into multicomponent glass fibres for use in optical communications [1]. In particular sodium borosilicate glasses drawn into fibre using double crucible techniques have been shown to give optical losses below 3.5 dB km^{-1} and bandwidths in excess of 300 MHz km [2]. These figures are close to those that can be obtained in doped fused silica fibres operating at 0.85 μm. It is, however, recognized that the strength of multicomponent glasses is significantly different to that of silica [3] and that the presence of an alkali component may well influence the durability and fatigue. Fatigue is normally characterized by the stress corrosion susceptability, N, and this parameter has a marked effect on the fibre lifetime [4]. This has been well documented for silica fibre and predictions of lifetime have been made for several service conditions [5].

In order that similar predictions can be made for multicomponent glass fibres, the strength and dynamic fatigue have been measured as a function of temperature and humidity. The results were used to estimate values of N. Zero stress ageing and static fatigue have also been measured and the effects of glass composition on these parameters has been determined.

2. Strength and dynamic fatigue

2.1. Fibre fabrication

All of the glasses used for this work were based on sodium borosilicates (designated by NBS). Either barium or germanium oxide was added to the core glasses to modify the refractive index and either aluminium, magnesium or zinc oxide added to the cladding glasses to improve durability. The fibre was drawn from a resistance heated platinum double crucible and was coated "in-line" with silicone resin. The coating techniques have been described in detail elsewhere [6]. A typical fibre diameter was 125 μm and this was kept constant to ± 1 μm by a diameter monitor and feedback loop.

2.2. Experimental procedures

Strength and dynamic fatigue measurements were made using a two point bending technique which has been previously reported [7]. Essentially a fibre sample is bent through 180° between two parallel jaws which are driven together at constant velocity. The fibre is bent to a smaller radius until it eventually fractures, and by measuring the jaw separation at the instant of fracture, the fibre strength can be determined. Since the effective gauge length is only about 0.5 mm, the probability of measuring a fibre sample containing a large

0022–2461/83/030785–08$03.46/0

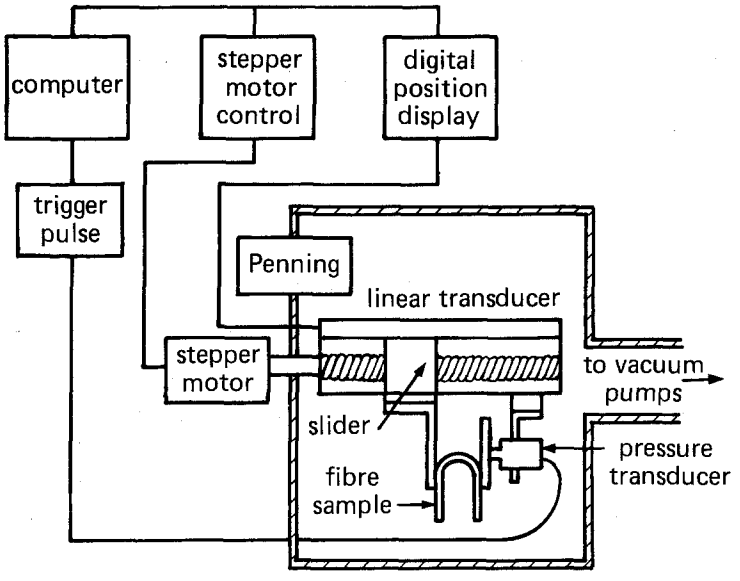

Figure 1 Two-point bending technique for measuring fibre strength.

flaw is very small and consequently the results tend to be uniform and unimodal.

The technique is ideally suited to measuring strengths in different environments since the fibre and jaws can easily be immersed in the environment of interest. More recently we have made measurements in vacuo by enclosing the entire apparatus in a vacuum chamber (Fig. 1).

2.3. Dynamic bending fatigue

Dynamic fatigue is conventionally measured by determining fibre strength as a function of rate of strain according to [4]:

$$s^{N+1} = B(N+1)\dot{s}S^{N-2} \qquad (1)$$

where s is the ambient strength, B is a material constant, $\dot{s}$ is the rate of applied stress and S is the inert strength. If log(s) is measured as a function of log ($\dot{s}$) then:

$$\log s = \frac{1}{N+1}\log \dot{s} + k \qquad (2)$$

so N can be determined from the slope of the graph, and k is the intercept.

However, in two point bending the jaws are closed together at constant velocity so that the applied rate of strain is not constant and consequently a modified dynamic fatigue equation must be derived. From the theory [3] it can be shown:

$$s^{N-1} = B(N-1)\frac{0.42}{E}\frac{V}{a}S^{N-2} \qquad (3)$$

where E is Young's Modulus, V is the jaw velocity and a is the fibre radius. From Equation 3 it can be seen that:

$$\log s = \frac{1}{N-1}\log\frac{V}{a} + k' \qquad (4)$$

hence the dynamic fatigue constant, N, can be determined by varying the velocity of the jaws, and k' is the new intercept.

2.4. Results

Fig. 2 shows the results of measuring dynamic fatigue in various environments. The fibre was made from a six component glass sytem (NMZABS) which is explained further in Section 3. At liquid nitrogen temperatures the measured strength was equivalent to 14% breaking strain (10 GPa) and N was very large. As the effective dew point of the

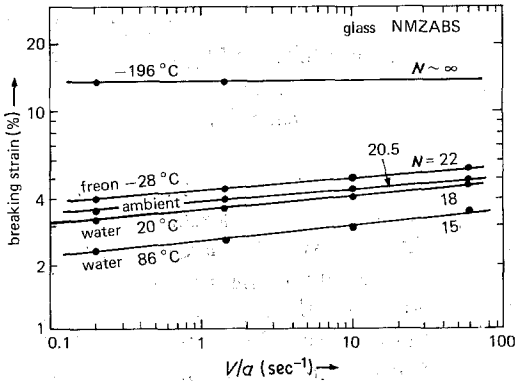

Figure 2 Dynamic fatigue of multicomponent glass.

environment was increased from − 28 to + 86° C then both the measured value of strength and the value of N decreased.

Fig. 3 shows in more detail the effects of temperature and humidity. Again the glass was a six component system (NMZABS) and each point was measured at a constant value of V/a (1.4 sec^{-1}). In order to make these measurements the fibre was immersed in a series of water-saturated liquids which could be maintained at the required temperature. For example, isopentane was used to cover the range − 140 to − 100° C, CCl_3F from − 100 to 0° C and deionized water from 0 to 100° C. Liquid nitrogen was of course used for − 196° C. Since the fibre was polymer coated, and since each liquid was saturated with water, the effective relative humidity at the polymer–glass interface was maintained at 100% r.h. If a non-saturated liquid was used, for example isopropanol which is miscible with water, then the effective humidity was much lower and high values of strength could be measured [3]. Effectively, therefore, since the fibre was maintained at 100% r.h. at each temperature, the temperature axis in Fig. 3 also corresponds to dew point.

In order to separate the effects of temperature from those of moisture content, a series of measurements were also made at room temperature *in vacuo*. The pressure was varied at 760 torr down to 10^{-5} torr and the results are also plotted on Fig. 3. As the pressure, and hence dewpoint, was reduced the fibre strength increased. These points are also replotted on the graph at their respective dewpoints and are shown as triangles (for example, a pressure of 10^{-5} torr corresponds to a dewpoint of − 110° C). The replotted measurements *in vacuo* agree well with the original curve and provide evidence that the increase in strength at low temperatures is a result of reducing the environmental moisture content.

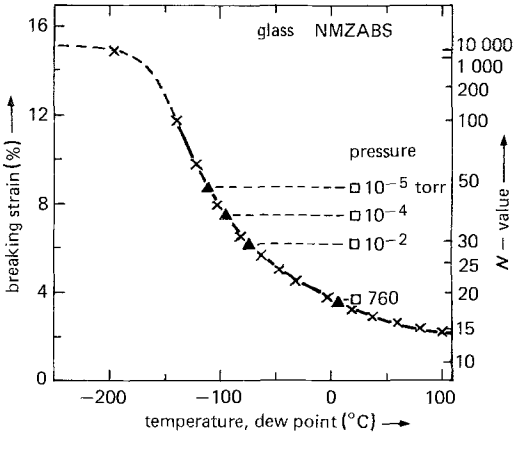

Figure 3 Variation of strength with temperature (dewpoint) and pressure. x measurements in water-saturated liquids. □ measurements *in vacuo*. △ replotted measurements *in vacuo*.

2.5. Discussion

From a consideration of Equation 3 it can be seen that the measured value of strength s depends on N. In other words changes in strength result from changes in the amount of stress corrosion occurring during measurement. This trend is confirmed by examining the dynamic fatigue data of Fig. 2. As N decreased the value of s also decreased. Since, we concluded in the previous section that strength depends on environmental moisture content, we can therefore further conclude that stress corrosion susceptibility, N, also depends on water content, rather than temperature.

At first sight this is surprising since it suggests that the activation energy required for stress corrosion of Si–O bonds is very low. However, consider the model by Weiderhorn [8], where crack velocity dc/dt is given by:

$$dc/dt = V_0 \exp(-E + bK_I)/RT \qquad (5)$$

where c is the crack depth, t is time, K_I is the stress intensity, R is the gas constant, T is temperature, and V_0, b and E are constants. The effective activation energy is $(E - bK_I)$ and is reduced at high values of K_I or, in other words, as the strain is increased. For dynamic fatigue measurements on strong fibre the levels of strain are in general fairly high and it is possible that this reduces the activation energy for stress corrosion to very small quantities.

Using Equation 3 the vertical axis of Fig. 3 can be recalibrated in terms of the N-value, as shown in the right-hand axis, and N is also determined as a function of dewpoint. Fig. 4 now shows how N varies with water content.

3. Effects of glass composition on ageing

Glass fibre can degrade as a result of surface attack from water, even when stored under zero stress, and glass compositions which maintain their initial high strength over long periods are being sought. With a view to this fibres were stored in distilled water at 20° C and their strengths were measured as a function of immersion time. The results are

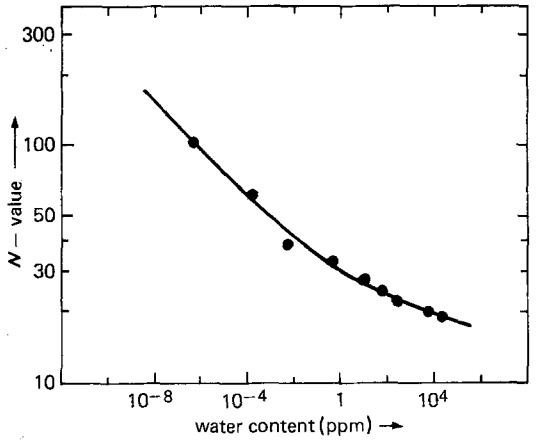

Figure 4 Variation of N-value with moisture content.

shown in Fig. 5 and depict glass compositions given in Table I. The glasses were based on sodium borosilicates with magnesium, aluminium and zinc oxide added in the region of 1 to 2 mol%. NBS (1) contained 25 mol% soda and NBS (2) only 20%. Sodium is of course a network modifier and it is generally recognized that reducing the modifier content results in improved durabilities. It has also been recognized from glass leaching studies [9] that small additions of materials such as alumina can have marked effects on glass durability. It is generally thought that this material forms an alumino–silicate layer at the surface of the glass which acts as a barrier for any further corrosion. The simultaneous addition of magnesium, aluminium and zinc oxides gives the most durable glass. Similar results have also been seen by Shibata *et al.* [10].

The degradation in fibre strength was irreversible and drying for several hours in dry nitrogen had no effect. Liquid nitrogen measurements made as a function of immersion time in water are shown in

TABLE I

Symbol	Composition
NBS (1)	Sodium borosilicate (high soda)
NBS (2)	Sodium borosilicate (low soda)
NBS (3)	Sodium borosilicate (low soda)
NABS	Sodium–aluminium borosilicate
NZABS	Sodium–zinc–aluminium borosilicate
NMZABS	Sodium–magnesium–zinc–aluminium borosilicate

Fig. 6 for NBS(3) glass, and compared with measurements made at ambient temperatures. The results confirm that ageing is caused by a reduction in inert strength and therefore by an increase in initial flaw size. The curve can be fitted to an equation of the form: $S = S_0(1 + \alpha t)^{-\beta}$, with $\alpha = 1.67 \times 10^{-4}$ sec^{-1} and $\beta = 0.222$.

Ageing effects under ambient conditions are shown in Fig. 7. Whereas the two sodium borosilicate glasses exhibit a small deterioration in strength, the four and six component glasses show virtually no change up to times approaching a year.

4. Static fatigue

4.1. Experimental details

Static fatigue, or delayed failure, is known to occur in most glasses and has been measured extensively in high-silica optical fibres [11]. Time to failure, t_f, has been found to obey the relationship [12].

$$t_f = BS^{N-2}\sigma^{-N} \qquad (6)$$

where σ is the applied constant stress.

Static fatigue measurements were made on multicomponent glass fibres using a mandrel technique [13]. A constant strain was applied to a coated fibre by wrapping it around a circular mandrel. The applied strain is given by:

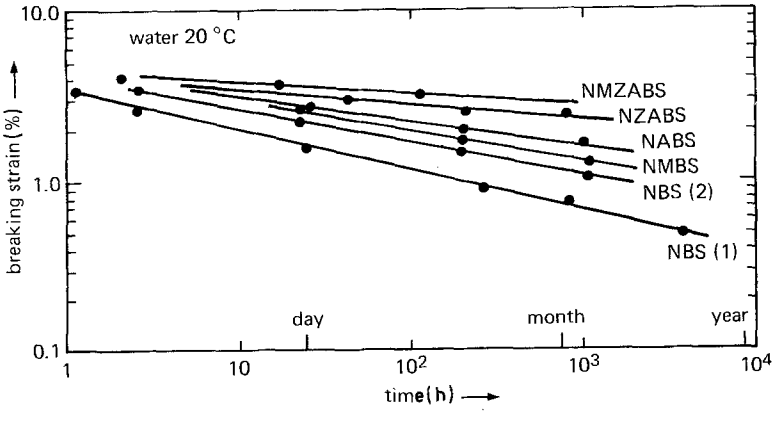

Figure 5 Zero stress ageing in water at 20° C.

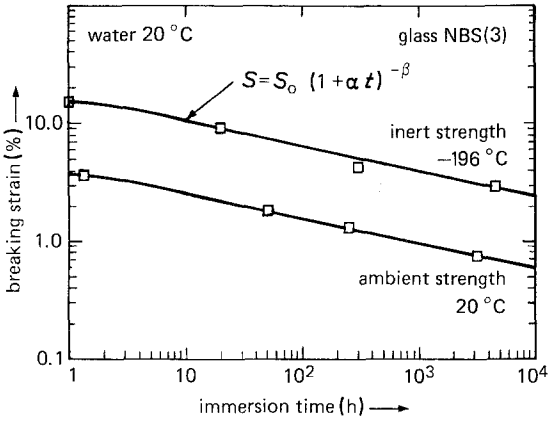

Figure 6 Comparison of inert (− 196° C) and ambient (20° C) strength measurements of fibre stored in water at 20° C under zero stress. The inert strength curve can be fitted to $S = S_0(1 + \alpha t)^{-\beta}$ with $\alpha = 1.67 \times 10^{-4}$ sec^{-1} and $\beta = 0.222$.

$$\tau = a/(a + t + R) \qquad (7)$$

where a is fibre radius, t is coating thickness and R is mandrel radius. In general 30 samples were set up at each strain and the time to failure was measured in each case. Providing the initial fibre strength was uniform, good results could be obtained using this method.

4.2. Results

Results from a four-component glass fibre (NABS) are shown in Fig. 8. Measurements were made in air (50% r.h.) and distilled water both at 20° C. Each line in Fig. 9 corresponds to a single value of strain and gives the time to failure for each of 30 samples. In principle, a value of N can be obtained directly from this graph since each line should have a slope of $m/N - 2$ [12], where m is the Weibull parameter from strength probability distributions. However since it is difficult to measure m directly, all that can be concluded is that $N(\text{air}) > N(\text{water})$.

Fig. 9 shows a static figure diagram for results in air at 20° C as a function of glass composition. The static fatigue Equation 6 appears to be valid for all compositions and N has values of around 20, agreeing with dynamic fatigue data from Section 2.

Static fatigue results in water at 20° C are shown in Fig. 10. In this case the data cannot be fitted to the usual fatigue equation, but exhibits a continual change in slope that is dependent on the glass composition. The incorporation of magnesium, aluminium and zinc oxides into the cladding glass significantly improves the fatigue behaviour, and the influence of composition showed similar trends to those evident in Section 3. (The arrow on the final NMZABS data point indicates that this set of fibres had not failed at the time of writing.) Similar effects have been reported in high-silica fibres [14].

5. Modified static fatigue theory

Although the departure from conventional stress-corrosion theory, evident in Fig. 10, could be explained by a continual change in N-value, the similarity of the compositional effects on static fatigue and zero-stress ageing, suggests that this departure is caused by a combination of stress corrosion and ageing. Further evidence for this is given in Fig. 11, which shows results for NBS (3) fibre. Since the curves are almost parallel this indicates that N is constant with time, despite large changes in the applied strain.

5.1. Crack growth caused by ageing

From the data in Fig. 6 it can be seen that for the case of NBS (3) the inert strength can be given as a function of time t according to:

$$S(t) = S_0(1 + \alpha t)^{-\beta} \qquad (8)$$

where $S(t)$ is inert strength and S_0 is initial inert strength. From the data $\alpha = 1.67 \times 10^{-4}$ sec^{-1} and $\beta = 0.222$. If we now postulate that zero-stress ageing is caused by the growth of surface

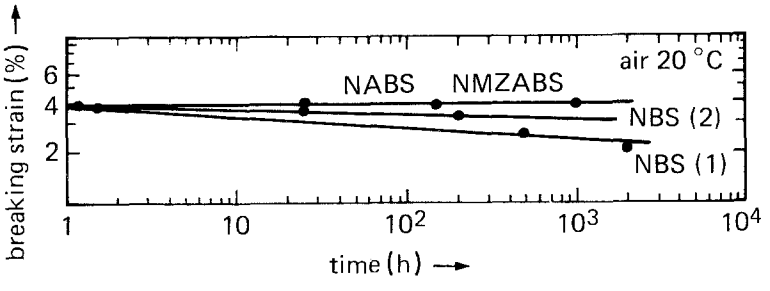

Figure 7 Zero stress ageing in air at 20° C and 50% r.h.

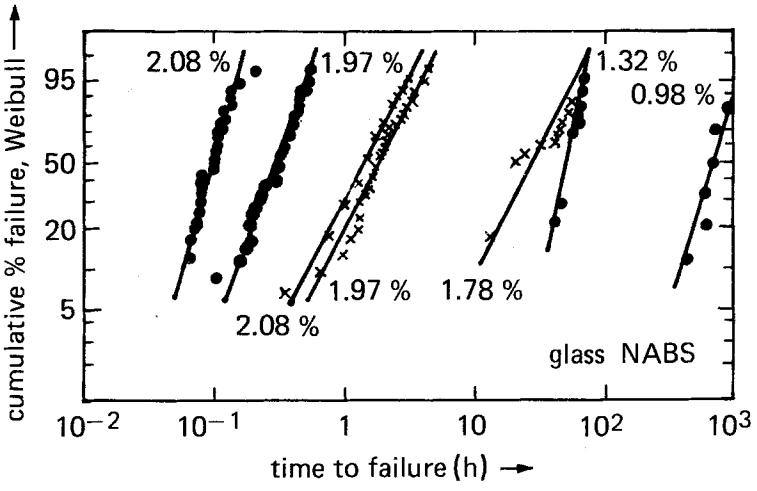

Figure 8 Static fatigue data of multicomponent glass fibre by mandrel testing: • results in 20° C water, x results in air.

flaws under attack by water, and that these flaws are similar to microcracks of depth c, then using:

$$K_{IC} = SYc^{1/2} \tag{9}$$

(where K_{IC} is the critical stress intensity factor and Y is a geometric factor depending on the flaw shape) we can deduce that:

$$c = c_0(1 + \alpha t)^{2\beta} \tag{10}$$

with

$$c_0 = K_{IC}^2/Y^2S_0^2 \tag{11}$$

where c_0 is initial crack depth at time zero.

Equation 10 now predicts the growth of flaws in multicomponent glasses caused by ageing, and the crack velocity can be derived to be:

$$\frac{dc}{dt} = \frac{2c_0\alpha\beta}{(1 + \alpha t)^{1-2\beta}}. \tag{12}$$

5.2. Crack growth due to stress corrosion

The theory of stress corrosion postulates that if stress is applied to a fibre in an atmosphere containing moisture, then a water molecule can diffuse into the crack and break-up the glass structure just at the tip of the crack where the stress is at its highest level. Empirically it has been found [15]:

$$\frac{dc}{dt} = AK_I^N \tag{13}$$

where A is a material constant and K_I is the stress intensity factor.

A solution of Equation 13 gives:

$$c = \frac{K_{IC}^2}{Y^2}\left(S^{N-2} - \frac{\sigma^N t}{B}\right)^{2/2-N} \tag{14}$$

which predicts crack growth due to stress corrosion.

5.3. Combination of ageing and stress corrosion

Crack growth behaviour in multicomponent glasses as predicted for both stress corrosion and zero stress ageing is shown in Fig. 12. This was

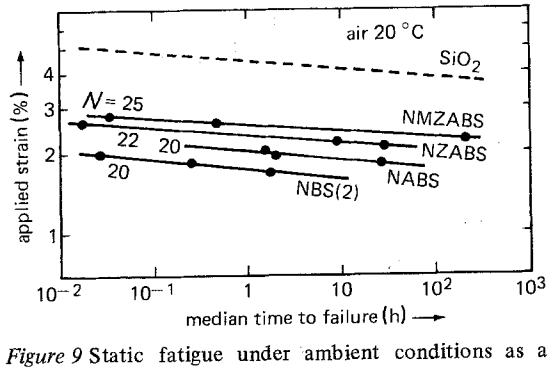

Figure 9 Static fatigue under ambient conditions as a function of glass composition.

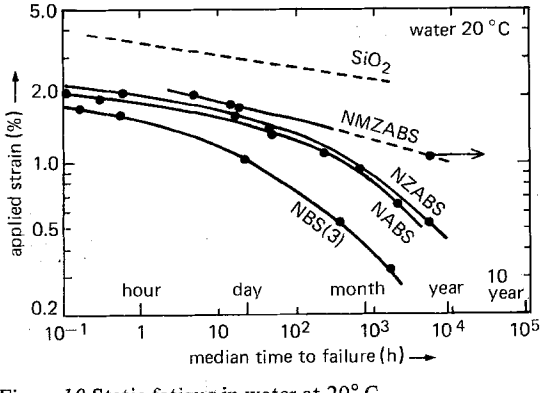

Figure 10 Static fatigue in water at 20° C.

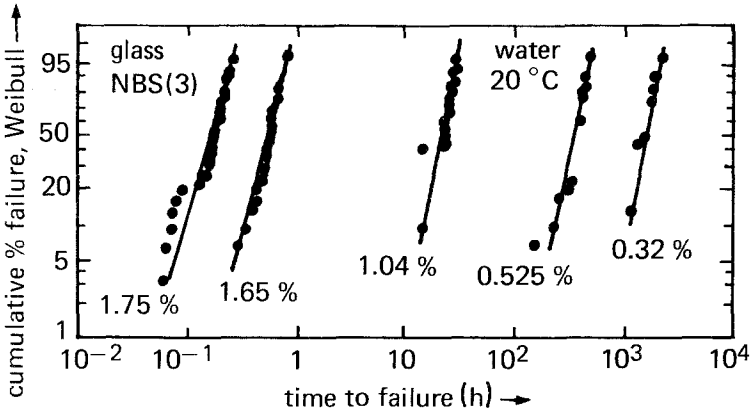

Figure 11 Static fatigue data for NBS glass fibre in water at 20° C.

determined from Equations 14 and 10, respectively. To obtain a complete solution to the case where these processes are combined it is necessary to solve:

$$\frac{dc}{dt} = AK_I^N + \frac{2c_0 \propto \beta}{(1+\alpha t)^{1-2\beta}} . \qquad (15)$$

It is difficult to obtain an analytical solution to this differential equation but an indication of the effects this will have on delayed failure can be obtained by considering Fig. 12. Whereas ageing leads to a steady but slow growth of cracks, stress corrosion is virtually negligible over the initial periods and only becomes significant at times close to t_f. For this study the case is considered where crack growth over the time interval $(0, t_f/2)$ is caused only by ageing and over the time interval $(t_f/2, t_f)$ is caused only by stress corrosion, and we then have the situation shown in Fig. 13.

Combining Equations 6 and 8, with $t = t_f/2$, we now obtain:

$$t_f[(1+\alpha t_f/2)^{\beta(N-2)}/2] = BS_0^{N-2}\sigma^{-N} \qquad (16)$$

which gives an approximate indication of the delayed failure behaviour after considering both stress corrosion and zero stress ageing. Using values of α and β from Fig. 6, it is possible to determine how t_f varies with the applied strain (σ) and this is shown in Fig. 14. The theoretical curve was plotted from Equation 16 assuming $N = 15$. The experimental static fatigue data from Fig. 10 is also shown in good agreement with the theoretical prediction.

At short time intervals the data tends asymptotically to the usual static fatigue cruve, implying that dynamic fatigue normally carried out over short time intervals should be valid even in samples that exhibit ageing. Moreover it also demonstrates that there is a clear correlation between the ageing

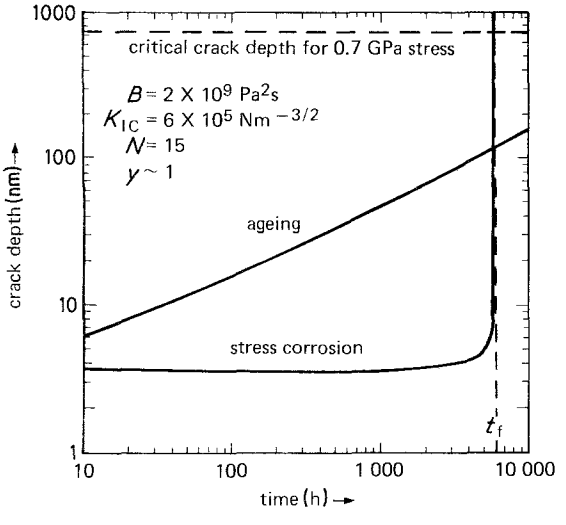

Figure 12 Crack depth as a function of time.

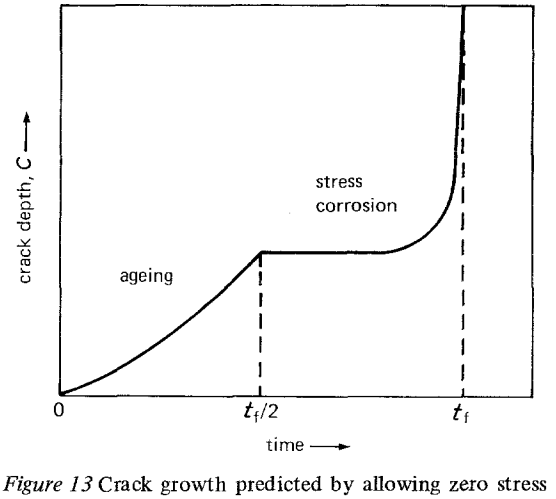

Figure 13 Crack growth predicted by allowing zero stress ageing up to time $t_f/2$ and stress corrosion up to time t.

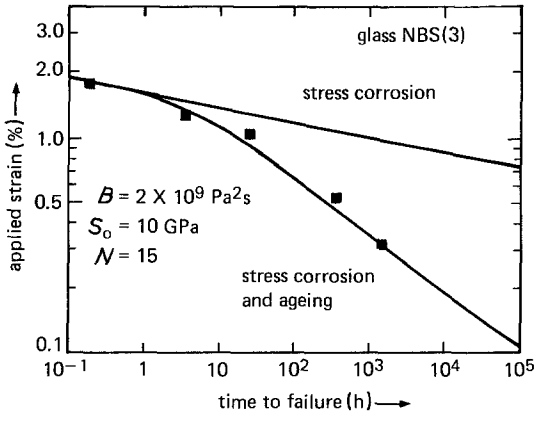

Figure 14 Modified static fatigue.

properties of a glass and its static fatigue behaviour. For example, NMZABS exhibited the best ageing and the best static fatigue properties and survived strains of greater than 1% for times of up to 10^4 h.

6. Conclusions

Strength and dynamic fatigue of multicomponent glass fibre were measured using a two-point bending technique. The measured value of strength was found to be related to the N-value and this could be varied by decreasing the dew-point of the measurement environment. At low-temperatures or equivalently in high vacuum both the fibre strength and the N-value increased, and the results suggest that fatigue is determined by environmental moisture content rather than absolute value of temperature.

Zero-stress ageing was measured in ambient air and in water at 20° C and the results were found to be strongly determined by glass composition. Static fatigue was also measured using a mandrel technique and similar compositional trends were evident. The addition of a few mole per cent of aluminium, magnesium and zinc oxides to sodium borosilicate glasses gave a significant improvement and a glass has been developed which could survive in water for up to 10^4 h at strains greater than 1%.

Finally a modified theory of static fatigue was outlined which combined the phenomena of zero-stress ageing and stress corrosion and predicted a departure from conventional stress corrosion theory that was evident in some glass compositions.

Acknowledgements

The authors would like to thank Dr Partington for preparing many of the glass compositions, J. Stefanie for helpful discussions on the theory, S. Craig for some of the measurements and the Director of Research, British Telecom, for permission to publish this paper.

References

1. K. J. BEALES, C. R. DAY, A. G. DUNN and S. PARTINGTON, *Proc. IEEE* **10** (1980) 1191.
2. K. J. BEALES, C. R. DAY, W. J. DUNCAN, A. G. DUNN, P. L. DUNN and G. R. NEWNS, *Phys. Chem. Glasses* **21** (1980) 25.
3. P. W. FRANCE, W. J. DUNCAN and K. J. BEALES, Proceedings of the 12th International Congress on Glass, Albuquerque, 1980 (North-Holland, Amsterdam).
4. J. E. RITTER, *Fiber Int. Optics* **1** (1978) 387.
5. W. J. DUNCAN, P. W. FRANCE and K. J. BEALES, Proceedings of the 7th European Conference on Optical Fibre Communication, Copenhagen, 1981 (Peter Peregrinus, Stevenage).
6. P. W. FRANCE, P. L. DUNN and M. H. REEVE, *Fiber Int. Optics* **2** (1979) 267.
7. P. W. FRANCE, M. J. PARADINE, M. H. REEVE and G. R. NEWNS, *J. Mater. Sci.* **15** (1980) 825.
8. S. M. WEIDERHORN and L. H. BOLZ, *J. Amer. Ceram. Soc.* **53** (1970) 543.
9. L. L. HENCH, *J. Non-cryst. Solids* **19** (1975) 27.
10. S. SHIBATA, S. TAKAHASHI, S. MITACHI and M. YASU, *ibid.* **43** (1981) 79.
11. D. KALISH and B. K. TARIYAL, *J. Amer. Ceram. Soc.* **61** (1978) 518.
12. *Idem, Appl. Phys. Lett.* **28** (1976) 721.
13. C. K. KAO, "Optical Fibre Communications" (John Wiley and Sons Ltd, Chichester 1980) p. 241.
14. J. T. KRAUSE, Proceedings of the 12th International Congress on Glass, Albuquerque, 1980 (North-Holland, Amsterdam) p. 497.
15. A. G. EVANS and S. M. WEIDERHORN, *Int. J. Fract.* **10** (1974) 379.

Received 14 May
and accepted 19 July 1982